Measurement of Ne 1s and 1snl satellite photoelectron spectra near threshold

L. Avaldi,[1] G. Dawber,[2] R. Camilloni,[1] G. C. King,[2] M. Roper,[3] M. R. F. Siggel,[3]
G. Stefani,[4] M. Zitnik,[5] A. Lisini,[6] and P. Decleva[6]
[1]*Istituto di Metodologie Avanzate Inorganiche del Consiglio Nazionale delle Ricerche, Area della Ricerca di Roma, Cassella Postale 10 00016 Monterotondo Scalo, Italy*
[2]*Department of Physics, Schuster Laboratory, Manchester University, Manchester M13 9PL, United Kingdom*
[3]*Science and Engineering Research Council, Daresbury Laboratory, Daresbury, Warrington WA4 4AD, United Kingdom*
[4]*Dipartimento di Fisica "E. Amaldi", III Università di Roma, Roma, Italy*
[5]*J. Stefan Institute, University of Ljubljana, Ljubljana, Slovenia*
[6]*Dipartimento di Scienze Chimiche, Università di Trieste, Via L. Giorgieri 1, 34127 Trieste, Italy*
(Received 27 December 1994)

Near-threshold inner-shell photoionization of neon has been studied by measuring threshold photoelectron spectra in the energy regions of the $1s^{-1}$ main line and the $1s2p^5nl$ satellite states. The measured linewidth (0.22 ± 0.03 eV) of the $1s \rightarrow 3p$ transition is more consistent with the observation of the 1s hole state linewidth than previous determinations. Features, assigned as doubly excited states and conjugate shakeup transitions, have been discerned in the $1s2p^5nl$ satellite spectrum.

PACS number(s): 32.80.Hd

The high sensitivity and energy resolution of threshold photoelectron spectroscopy (TPES) have made this technique a unique tool to study photoionization of valence and inner valence shells of atoms [1–3] and molecules [4–6]. Recently, the application of TPES has been extended to the photoionization of inner shells of the rare gases [7,8] and small molecules [9,10]. This paper describes the observation of Ne 1s and 1snl threshold photoelectron spectra. To our knowledge, the only experiment that previously approached the Ne 1s threshold is the one by Kobrin *et al.* [11], who studied the relative intensities of the main line and its satellites from 7 to about 50 eV above their respective thresholds. X-ray photoelectron spectra of the Ne 1s main line and its satellites have been reported by several authors [12,13], and recently studied again using monochromatic x-ray excitation [14]. The energy region of the Ne *K*-shell edge has also been investigated by photoabsorption [15–20] and electron-energy-loss spectroscopy [21] (EELS).

The present experiment has been performed at the Daresbury Laboratory Synchrotron Radiation Source, where a high-resolution threshold spectrometer has been allied to the 5U1 undulator beam line. This beam line provides radiation in the energy range 70–1500 eV with a resolving power and a photon flux close to the Ne *K*-edge of ≈ 1300 and 10^{11} photons/sec, respectively [22,23]. The photoelectron spectrometer has been described in detail elsewhere [24]. A draw-out field, applied between the target region and the entrance to the lens stack of the analyzer, collects very-low-energy electrons with high efficiency over 4π *sr* and discriminates against high-energy electrons. The threshold energy resolution of the spectrometer is better than 10 meV [24], i.e., we are able to study excitation of the ion states within this value of their thresholds.

In Fig. 1, the threshold photoelectron spectrum of Ne in the region of the 1s main line is shown. Despite the low Ne 1s cross section close to threshold (~ 0.3 Mb [25]) the count rate of the Ne 1s main line was 800 sec^{-1} and the total accumulation time for this spectrum was only 10 min.

The lowest-energy peak observed in Fig. 1, assigned to the dipole allowed $1s \rightarrow 3p$ transition, has been used to calibrate the photon energy scale [21]. The observation of a peak due to excitation of a 1s electron into an unoccupied state in the spectrum of zero kinetic-energy electrons, can arise either because of a shake-off decay $[Ne^*(1s^22s^22p^63p) \rightarrow Ne^{2+}(1s^22s^22p^4) + \varepsilon l \varepsilon' l']$ of the core excited states, where the two final electrons share the excess energy, or because of a two-step mechanism $[Ne^*(1s^22s^22p^63p) \rightarrow Ne^{+*}(1s^22s^22p^4np) + \varepsilon l \rightarrow Ne^{2+} + \varepsilon' l'(E_K = 0)]$, where the singly charged state, generated in the decay of the core excited state, is almost degenerate with a Ne^{2+} state. According to the more recent high-resolution photoelectron spectroscopy studies of the Ne^{+*} satellites [2,3,26] this coincidence seems unlikely. Therefore, the first mechanism is expected to be the main one responsible for the observed peak.

While in photoabsorption [19,20] and EELS [21] the peak due to the $1s \rightarrow 3p$ transition was observed to dom-

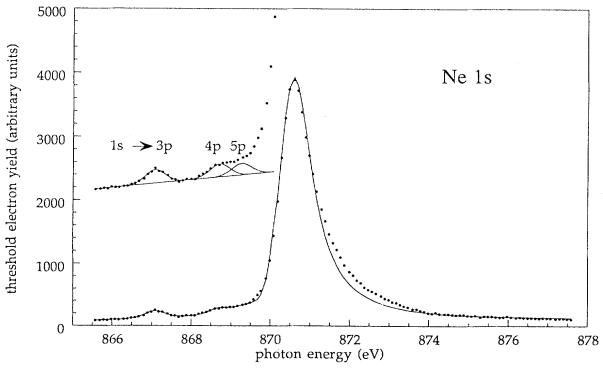

FIG. 1. Threshold photoelectron spectrum in the region of the neon *K* ionization limit. A PCI line shape [33] has been fitted to the Ne $1s^{-1}$ main line. In the inset the fit with a series of Gaussian functions to the $1s \rightarrow np$ ($n \geq 3$) transitions below the Ne $1s^{-1}$ threshold is shown.

inate the spectrum, in the threshold spectrum it is only a small percentage of the total intensity observed. This is consistent with the mechanism proposed above because Aksela *et al.* [27] observed that the $1s2s^22p^6$ and $1s2s^22p^63p$ hole states decay with a probability of about 98.2% by Auger transitions. Therefore, only less than 2% of the inner-shell excited states may decay via a double shake-off with a low-energy electron and contribute to the peak observed in the threshold spectrum. From the observed full width half maximum (FWHM) of 0.59 ± 0.04 eV a natural linewidth of 0.22 ± 0.03 eV has been derived for the $1s\rightarrow3p$ transition. This value is in agreement with the most recent determination of 0.23 eV [20] in a photoabsorption measurement and is consistent with the predicted (0.25 eV [28]) and measured [13,14] linewidth of the $1s$ hole state. This confirms the continuity between the properties of the higher excited Rydberg states and the inner hole state [29], questioned in the case of Ne $1s$ by earlier photoabsorption [17,18] and EELS [21] measurements.

The broad feature on the low-energy side of the $1s$ main line is attributed to the $1s\rightarrow np\,(n>3)$ core excited states. The experimental spectrum in this region has been simulated by two separate Gaussian peaks, which represent the $1s\rightarrow4p,5p$ transitions, and a series of closely spaced peaks of the same FWHM (0.6 eV) to represent the Rydberg states of higher quantum number. The results of this simulation are reported in Table I with previous determinations and are shown in the inset of Fig. 1.

The Ne $1s$ main line is broadened and shifted to higher photon energy by the post collision interaction (PCI) between the slow photoelectron and the faster Auger electrons, emitted in the decay of the inner hole. Among the several PCI theories [30–33] we have compared the present results with the one of van der Straten, Morgenstern, and Niehaus [32]. In an experiment where the collection energy, E, of the photoelectron analyzer is kept fixed and $h\nu$ is scanned, the probability that a photoelectron emitted with an initial energy E_{ph} will lose an amount of energy $\varepsilon=E_{ph}-E$, due to PCI has to be evaluated. Moreover, it is necessary to account for all the Auger decay channels of the inner hole. In order to compare the observed threshold spectrum with the theoretical predictions, the theoretical line shape [32] has been calculated (i) by changing the initial photoelectron energy E_{ph} at every value of $h\nu$, (ii) by accounting for the various Ne KLL transitions [34], and (iii) by assuming an isotropic distribution for the Auger electrons. The resultant line shape has been convoluted with a Gaussian function, which represents the apparatus function and then fitted to the experiments. The natural width Γ, the FWHM of the apparatus function and the height of the peak have been taken as free parameters. The best representation of the experiment has been obtained for $\Gamma=0.25\pm0.03$ eV and FWHM $=0.55\pm0.05$ eV. The experimentally measured shift is 0.47 ± 0.05 eV which compares with the theoretical prediction of 0.57 eV. Some differences are observed between the calculated and experimental shapes on the tail of the Ne $1s$ line. However it is impossible to ascertain if this is due to a shortcoming of the theory or to a too crude apparatus function used in the convolution procedure.

TABLE I. Measured energies for the observed transitions in the region of the Ne $1s$ ionization limit. The numbers in parentheses show the uncertainties in the last significant figure. The energy errors shown in the table do not contain the calibration errors.

Transition	Energy (eV) Ref. [21]	Ref. [19]	Others	Present work
$1s\rightarrow3s$	865.1(1)			
$1s\rightarrow3p$	867.05(8)	867.13(5)	867.07 (Ref. [16]) 867.09 (Ref. [17])	867.13[a]
$1s\rightarrow4p$	868.68(10)	868.77		868.76(5)
$1s\rightarrow5p$	869.23(15)	869.37		869.33(5)
$1s\rightarrow6p$	869.63(15)	869.65		
IP	870.1(2)	870.17	870.31(2) (Ref. [12])	870.07(5)[b]

[a]The energy of this transition has been used to calibrate the photon energy scale.

[b]This value is obtained from the measured position of the photoelectron peak and the calculated PCI shift.

The threshold photoelectron spectrum in the region of the $1s2p^5nl$ satellite states is shown in Fig. 2. The energy scale has been calibrated against the position of the $Ne^+(1s^{-1})$ main line (870.64 eV) where the assumption has been made that both the satellite and main peaks suffer the same PCI shifts. This is equivalent to assuming that the presence of a spectator electron does not alter significantly the Auger decay width of the inner hole, which is the main atomic parameter affecting the PCI shifts.

In the upper part of Fig. 2(a) are shown the energies of the $2p$-np shakeup transitions reported by Martensson, Svensson, and Gelius [14] in their x-ray photoelectron spectroscopy (XPS) measurements. The $2p$-np shakeup states form two series, known as the lower (L) and upper (U) series. This is due to the fact that in the final state there are three open shells. The $1s$ electron can first couple to the $2p$ electron as a triplet (lower) or a singlet (upper) parent state [14], which is then coupled to the np electron to form a ^2S shakeup state. In Fig. 2(a) the $2p$-$3p$ and -$4p$ members of the lower series and the first member $2p$-$3p$ of the upper one can be easily discerned. At higher energy some features of the spectrum may be assigned to the $2p$-$5p$ and $6p$ members of the lower series and to the $2p$-$4p$ member of the upper series. However, the spectrum in Fig. 2(a) displays more features than the XPS one. A broad feature, labeled "*a*", is observed at ≈31.7 eV followed by a tiny peak, labeled "*c*", at ≈33.4 eV; other structures, labeled "*b*", clearly appear on the low-energy flank of the $3p\,(L)$ peak and a rising continuum electron yield is observed well below the $Ne^{2+}(1s2p^5)$ threshold. Further features seem to contribute to the shakeup spectrum between 42 and 45 eV. Gelius [13] and Martensson, Svensson, and Gelius [14] have located the first conjugate shakeup transition at 33.35 ± 0.04 eV, while Esteva *et al.* [18] identified two $1s2s^22p^53p^2$ doubly excited states at 31.7 and 34.7 ± 0.1 eV.

In order to interpret the observed spectrum and the differences with the XPS one we have calculated the spectrum of the doubly excited states at the zero-order $2p$-$2h$

configuration-interaction (CI) level and the spectrum of the satellite states with the quasidegenerate perturbation theory within the CI approach (QDPT-CI). The details of the theoretical framework, which joins the flexibility of the CI approach with an accurate treatment of the residual dynamical correlations, have been reported elsewhere [35,36]. The first doubly excited state appears at ≈ 26 eV above threshold and then the density of states becomes very high, covering the full energy range explored. The energy position of the transitions with an intensity that is at least 1% of the one of the $1s \rightarrow 3p$ transition are reported in Fig. 2(b) and in the Table II. In the same figure also the positions of the transitions belonging to the $2p^5ns$ and $np(^2P)$, $2p^5np$ and $nd(^2D)$, $2p^5ns$ and $np(^2P)$, and $2p^5nd(^2F)$ conjugate shakeup series are shown. The positions of the states belonging to the $2p^5np(L)$ and (U) series are not reported because they are in very good agreements with the XPS observations.

The features *a* and *b* can be definitely assigned to doubly excited states. The assignment of peak *a* as the first of the $1s2s^22p^53p^2$ states is in agreement with the proposed assignment by Esteva *et al.* [18], while for the feature *b*, which in our spectrum appears as a double shoulder, we propose the $1s2s^22p^53p4p$ and $3s3d$ states for the lower-energy side and the $1s2s^22p^53p5p$ and $3s4d$ for the other part. The second $1s2s^22p^53p^2$ state is located under the $2p^53p(L)$ peak.

A doubly excited state may produce a peak in the threshold electron spectrum either if it is degenerate with a singly charged state, as observed in the inner valence region [2], or if it decays to the double ionization continuum via double shake off. By analogy with the decay route of the $1s \rightarrow np$ excited states, this latter mechanism appears to be the main mechanism responsible for features *a* and *b*.

The small feature *c* can be assigned to the $2p$-$3s$ conjugated shakeup transition. A conjugate shakeup transition involves a monopole transition of the inner electron into the continuum ($1s \rightarrow \varepsilon s$), while the valence electron undergoes a dipole transition ($2p \rightarrow ns$). In many-body perturbation theory (MBPT) [37–40], conjugate shakeup is explained in terms of a Coulomb interaction between the electron in the continuum and the valence electrons. Ishihara, Mizuno, and Watanabe [37] have calculated the ratio of the conjugate skakeup cross section to the $1s$ photoionization one versus the energy of the ejected photoelectron. This calculation predicts a ratio that increases from 0.05% at about 800 eV above threshold, in agreement with XPS observations, to 5% between 5 and 10 eV above threshold and then decreases to about 4.5% at threshold. In our spectrum the relative intensity of the conjugate shakeup to the $1s$ main line is $\leq 0.5 \pm 0.2\%$. This finding is consistent with the observation by Kobrin *et al.* [11], who did not observe any conjugate shakeup peaks at 7 eV above threshold and concluded that such a peak must have had a relative intensity less than 0.9%, and indicates that MBPT is overestimating the ratio when approaching its threshold.

The increased density of states that is predicted above 39 eV may lead to an explanation of the rising continuum yield in this region in terms of an envelope of unresolved states. Moreover the $2p$-$3d,5d\ ^2P, ^2D$ and ^2F and $2p$-$4s\ ^2P$ states might be responsible for the features located near the $2p$-$5p,6p(L)$ satellites. A deconvolution of the spectrum into individual lines to extract the intensity of each satellite relative to the $1s$ main line is unrealistic. However, to obtain an estimate of the intensity of the first members of the lower and upper series we have fitted a series of Gaussian functions of fixed FWHM, superimposed to a third degree polynomial, to represent the closely spaced unresolved features, to the experimental spectrum over the region 34–43 eV. The energy positions and the intensities of the $2p$-$3p$ and $4p(L)$ and $2p$-$3p(U)$ satellites are reported in Table III. Intensities lower than in the XPS spectrum [14] have been observed for all the features. A decrease of the relative intensity of

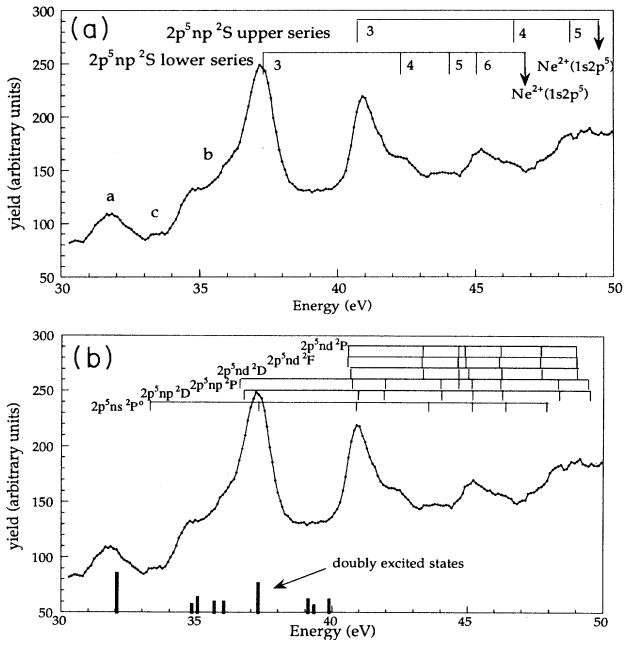

FIG. 2. Threshold photoelectron spectrum in the region of Ne^+ $1s2p^5nl$ states. The energy step in this spectrum is 100 meV per channel and the data accumulation time was ≈ 2 h. The energy scale is relative to the measured energy of the Ne $1s^{-1}$ main line. The energies of the members of $2p^5nl$ lower and upper series determined by XPS [14] are shown on the top of Fig. 2(a), while the QDPT-CI calculated energies of the ^2P, ^2D, and ^2F satellites as well as the calculated energies of the doubly excited states are displayed in Fig. 2(b).

TABLE II. Energies and assignments of Ne $1s2s2pnln'l'$ doubly excited states calculated at the zero-order $2p$-$2h$ CI level. Only states with intensities $\geq 1\%$ of the one of the $1s \rightarrow 3p$ transition are reported. The energy is relative to the $1s \rightarrow 3p$ transition.

Energy (eV)	Assignment
35.55	$1s2s^22p^53p^2$
38.30	$1s2s^22p^53p4p$
38.54	$1s2s^22p^53s3d$
39.13	$1s2s^22p^53p5p$
39.49	$1s2s^22p^53s3d$
40.74	$1s2s^22p^53p^2$
42.61	$1s2s^22p^53p4p$
42.78	$1s2s^22p^54p^2$
43.39	$1s2s^22p^53p5p$

TABLE III. Ne^+ $2p$-np satellite energies and intensities. The energy is relative to the Ne $1s^{-1}$ main line.

	Present work		XPS (Ref. [14])		Ref. [11]
Transition	Energy	Relative Intensity	Energy	Relative Intensity	Relative Intensity
$2p$-$3p(L)$	37.22	2.3(1)	37.3	3.27(6)	2.5(2)
$2p$-$4p(L)$	42.31	0.9(1)	42.3	1.9(2)	
$2p$-$3p(U)$	40.96	2.7(1)	40.7	3.15	3.0(2)[a]

[a]In Ref. [11] this is the sum of the intensities of the $2p$-$4p(L)$ and $2p$-$3p(U)$ states.

the shakeup satellites was also observed in the measurements of Kobrin *et al.* [11] and it is consistent with the findings of several threshold experiments on the inner valence shell of all the rare gases [2,3,41].

In summary, we have observed the Ne $1s$ and $1snl$ satellite photoelectron spectra at their respective thresholds. The present results enabled us to determine a value of the $1s \rightarrow 3p$ linewidth which is more consistent with the observation of the $1s$ hole state linewidth and with the observations in the other rare gases than previous determinations. Features attributed to inner-shell doubly excited and conjugate shakeup states have been discerned in the $1s2p^5nl$ satellite spectrum. The relative intensity of the $1s$-$3s$ conjugate shakeup to the $1s$ main line shows that MBPT is largely overestimating this ratio close to threshold.

This work has been partially supported by EEC Large Scale Installation Programme (Minor Grant No. 21/275). One of us (G.D.) thanks the British Council for a travel grant.

[1] W. B. Peatman, G. B. Kasting, and D. Wilson, J. Electron Spectrosc. Relat. Phenom. **7**, 233 (1975).
[2] R. I. Hall, G. Dawber, K. Ellis, M. Zubek, L. Avaldi, and G. C. King, J. Phys. B **24**, 4133 (1991).
[3] F. Heiser, U. Hergenhahn, J. Viefhaus, K. Williczek, and U. Becker, J. Electron Spectrosc. Relat. Phenom. **60**, 337 (1992).
[4] W. B. Peatman, J. Chem. Phys. **64**, 4368 (1976).
[5] K. Muller-Dethlefs and F. W. Schlag, Ann. Rev. Chem. **42**, 109 (1991).
[6] K. Ellis, R. I. Hall, L. Avaldi, G. Dawber, A. McConkey, L. Andric, and G. C. King, J. Phys. B **27**, 3415 (1994).
[7] L. Avaldi, G. Dawber, R. Camilloni, G. C. King, M. Roper, M. R. F. Siggel, G. Stefani, and M. Zitnik, J. Phys. B **27**, 3953 (1994).
[8] F. Heiser, S. B. Whitfield, J. Viefhaus, U. Becker, P. A. Heimann, and D. A. Shirley, J. Phys. B **27**, 19 (1994).
[9] P. A. Heimann, L. J. Medhurst, M. R. F. Siggel, D. A. Shirley, C. T. Chen, Y. Ma, and F. Sette, Chem. Phys. Lett. **183**, 234 (1991).
[10] L. J. Medhurst, P. A. Heimann, M. R. F. Siggel, D. A. Shirley, C. T. Chen, Y. Ma, S. Modesti, and F. Sette, Chem. Phys. Lett. **193**, 493 (1992).
[11] P. H. Kobrin, S. Southworth, C. M. Truesdale, D. W. Lindle, U. Becker, and D. A. Shirley, Phys. Rev. A **29**, 194 (1984).
[12] T. D. Thomas and R. W. Shaw, J. Electron Spectrosc. **5**, 1081 (1974).
[13] U. Gelius, J. Electron Spectrosc. **5**, 985 (1974).
[14] N. Martensson, S. Svensson, and U. Gelius, J. Phys. B **20**, 6243 (1987).
[15] J. Backovsky, Czech. J. Phys. **4**, 150 (1954).
[16] R. J. Liefield, Appl. Phys. Lett. **7**, 276 (1965).
[17] F. Wuilleumier, C. R. Acad. Sci. Paris **B270**, 825 (1970).
[18] J. M. Esteva, B. Gauthé, P. Dhez, and R. C. Karnotak, J. Phys. B **16**, L263 (1983).
[19] M. Domke, T. Mandel, A. Puschmann, C. Xue, D. A. Shirley, G. Kandl, H. Petersen, and P. Kuske, Rev. Sci. Instrum. **63**, 80 (1992).
[20] C. M. Teodorescu, R. C. Karnotak, J. M. Esteva, A. ElAlif, and J. P. Connerade, J. Phys. B **26**, 4019 (1993).
[21] A. P. Hitchock and C. E. Brion, J. Phys. B **13**, 3269 (1980); R. N. S. Sodhi and C. E. Brion, J. Electron Spectrosc. Relat. Phenom. **34**, 363 (1984).
[22] C. S. Mythen, G. van der Laan, and H. A. Padmore, Rev. Sci. Instrum. **63**, 1313 (1992).
[23] M. Roper (private communication).
[24] R. I. Hall, A. McConkey, K. Ellis, G. Dawber, L. Avaldi, M. A. MacDonald, and G. C. King, Meas. Sci. Technol. **3**, 316 (1992).
[25] J. J. Yeh and I. Lindau, At. Data Nucl. Data Tables **32**, 1 (1985).
[26] M. Pahler, C. D. Caldwell, S. J. Schaphorst, and M. O. Krause, J. Phys. B **26**, 1617 (1993).
[27] H. Aksela, S. Aksela, J. Tullki, T. Aberg, G. M. Bancroft, and K. H. Tan, Phys. Rev. A **39**, 3401 (1989).
[28] O. Keski-Rahkonem and M. O. Krause, At. Data Nucl. Data Tables **14**, 139 (1974).
[29] G. C. King, M. Tronc, F. H. Read, and R. C. Bradford, J. Phys. B **10**, 2479 (1977).
[30] A. Russek and W. Mehlhorn, J. Phys. B **19**, 911 (1986).
[31] F. H. Read and P. Hammond, J. Phys. B **21**, 4225 (1988).
[32] P. van der Straten, R. Morgenstern, and A. Niehaus, Z. Phys. **D8**, 35 (1988).
[33] M. Yu. Kuchiev and S. A. Sheinerman, Usp. Fiz. Nauk **158**, 353 (1989) [Sov. Phys. Usp. **32**, 569 (1989)].
[34] M. O. Krause, T. A. Carlson, and W. F. Moddeman, J. Phys. **32**, C4-139 (1971).
[35] A. Lisini and P. DeCleva, Chem. Phys. **171**, 1 (1992).
[36] A. Lisini, P. DeCleva, and G. Fronzoni, Chem. Phys. Lett. **209**, 135 (1993).
[37] T. Ishihara, J. Mizuno, and T. Watanabe, Phys. Rev. A **22**, 1552 (1980).
[38] J. Tulkki, Phys. Rev. Lett. **62**, 2817 (1989).
[39] T. M. Luke, J. D. Tolman, H. Aksela, and M. Levasalmi, Phys. Rev. A **41**, 1350 (1990).
[40] G. B. Armen, B. I. Crig, F. P. Larkins, and J. A. Richards, J. Electron Spectrosc. Relat. Phenom. **51**, 183 (1990).
[41] R. I. Hall, L. Avaldi, G. Dawber, P. M. Rutter, M. A. MacDonald, and G. C. King, J. Phys. B **27**, 3205 (1989).